TURKISH CLOUD RADIATION DATABASE (CRD) AND ITS APPLICATION BY USING CDRD BAYESIAN PROBABILITY ALGORITHM

[1]ÖZTOPAL A., [2]MUGNAI A., [2]CASELLA D., [2]FORMENTON M., [2]SANÒ P., [3]SÖNMEZ İ, [4]ŞEN Z., [5]KAYMAK M.K.

[1]İstanbul Technical University (ITU), Meteorological Department, İstanbul, Turkey

[2]Istituto di Scienze dell'Atmosfera e del Clima (ISAC), Consiglio Nazionale delle Ricerche (CNR), Roma, Italy

[3]Turkish State Meteorological Service (TSMS), Remote Sensing Division, Ankara, Turkey

[4]İstanbul Technical University (ITU), Hydraulic Division, İstanbul, Turkey

[5]Turkish State Meteorological Service (TSMS), Sabiha Gokcen Airport, Istanbul, Turkey

PRESENTATION OUTLINE

1. Climate Structure in Turkey
2. Observation Network in Turkey for This Study
3. Defense Meteorological Satellites Program (DMSP)
4. Establishment of CRD Database for Turkey
5. Analysis Procedure of Turkish CRD Database
6. The CDRD Retrieval Algorithm
7. Application and Results

WHAT IS THE CHALLENGING TASK HERE?

To determine ground rainfall amounts from few Special Sensor Microwave Imager/Sounder (SSMI/S) channels on DMSP Polar Satellite.

DMSP: Defense Meteorological Satellites Program

WHY IS IT DIFFICULT?

Ground rainfall cannot be observed from the space directly

BUT

the cloud physics helps to estimate the amount of ground rainfall

SO…

Cloud Radiation Database (CRD) is necessary to estimate the amount of ground rainfall by using Cloud Dynamic Radiation Database (CDRD) Retreival Algorithm

SSMI/S includes so much information about the atmospheric structure

BUT

it cannot provide cloud micro-physical structural information

SO...

for the rainfall algorithms we need external data source to obtain cloud micro-physical properties

Cloud Resolving Model (CRM) gives us the micro-physical properties.

In addition to all available data

micro-physical properties obtained from Radiative Transfer Model (RTM) help to determine the SSMI/S brightness temperatures (TBs), which can then be correlated with Cloud-Radiation Database (CRD) data generation

CDRD Bayesian probability algorithm combines the two sets of data

SSMI/S satellite data and CDR provide a common basis for rainfall prediction procedure through CDRD Bayesian probability algorithm,

CLIMATE STRUCTURE IN TURKEY

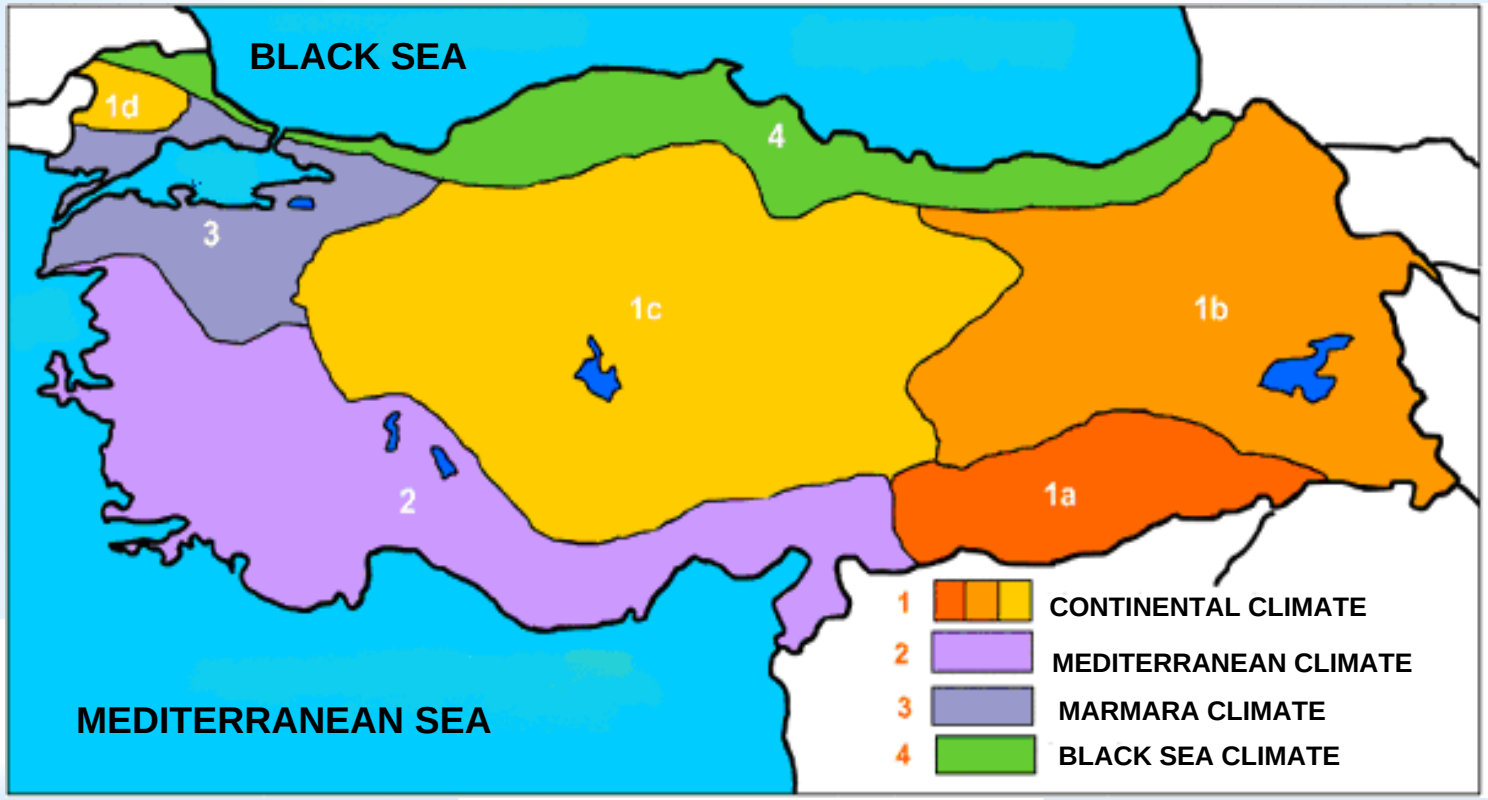

1) Continental climate (a, b, c and d): Temperature differences between winter and summer seasons is rather high; precipitation takes place frequently in winter and spring seasons and during summer dry spells occur. Depending on the precipitation and temperature features continental climate has four versions.

CLIMATE STRUCTURE IN TURKEY

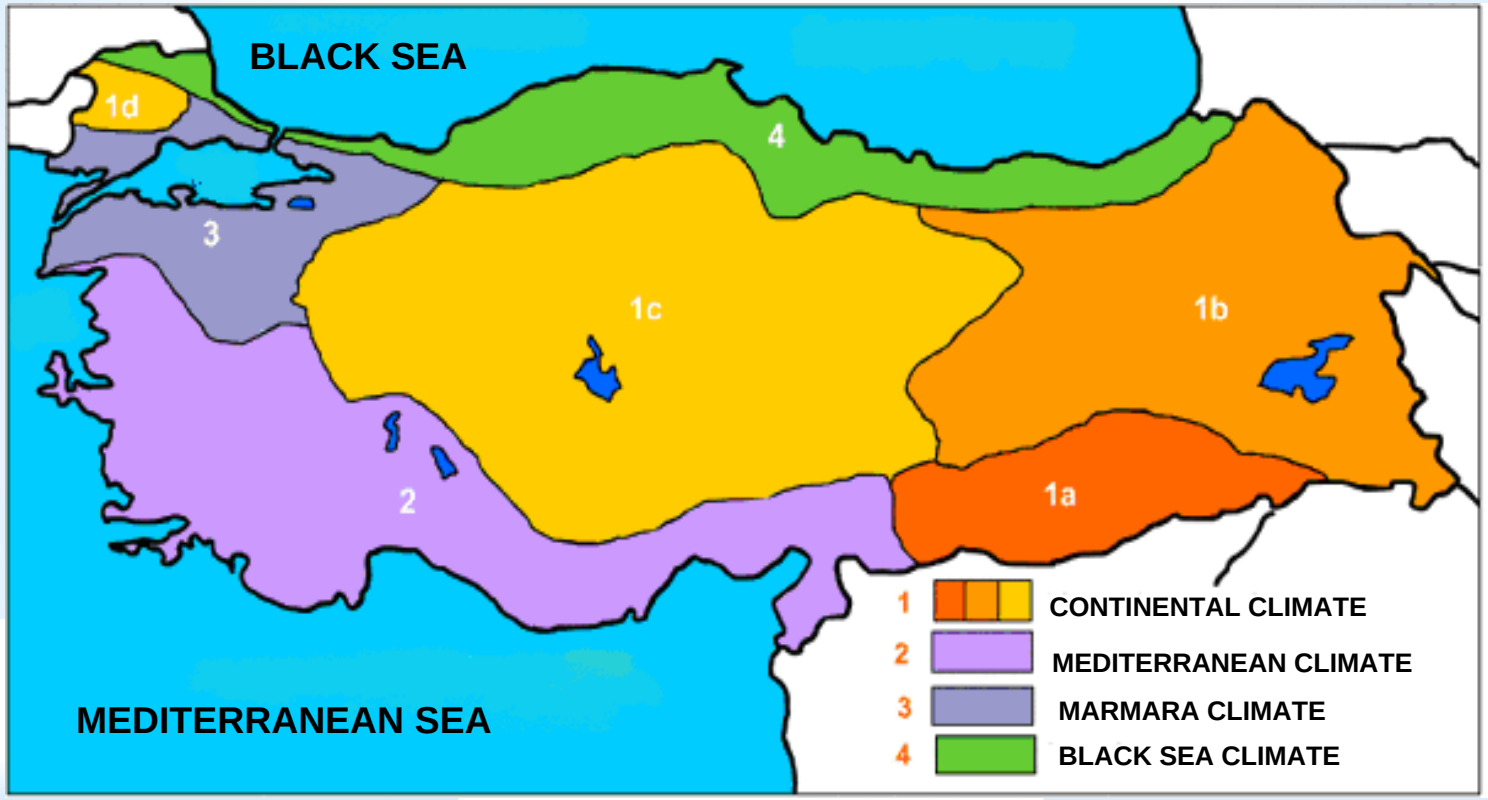

2) Mediterranean Climate: Summers are hot and dry but in winters warmair with heavy precipitation exists. Hail and snow fall events are scarce along the coastal regions. However, at high elevations winters are snowy and cold.

CLIMATE STRUCTURE IN TURKEY

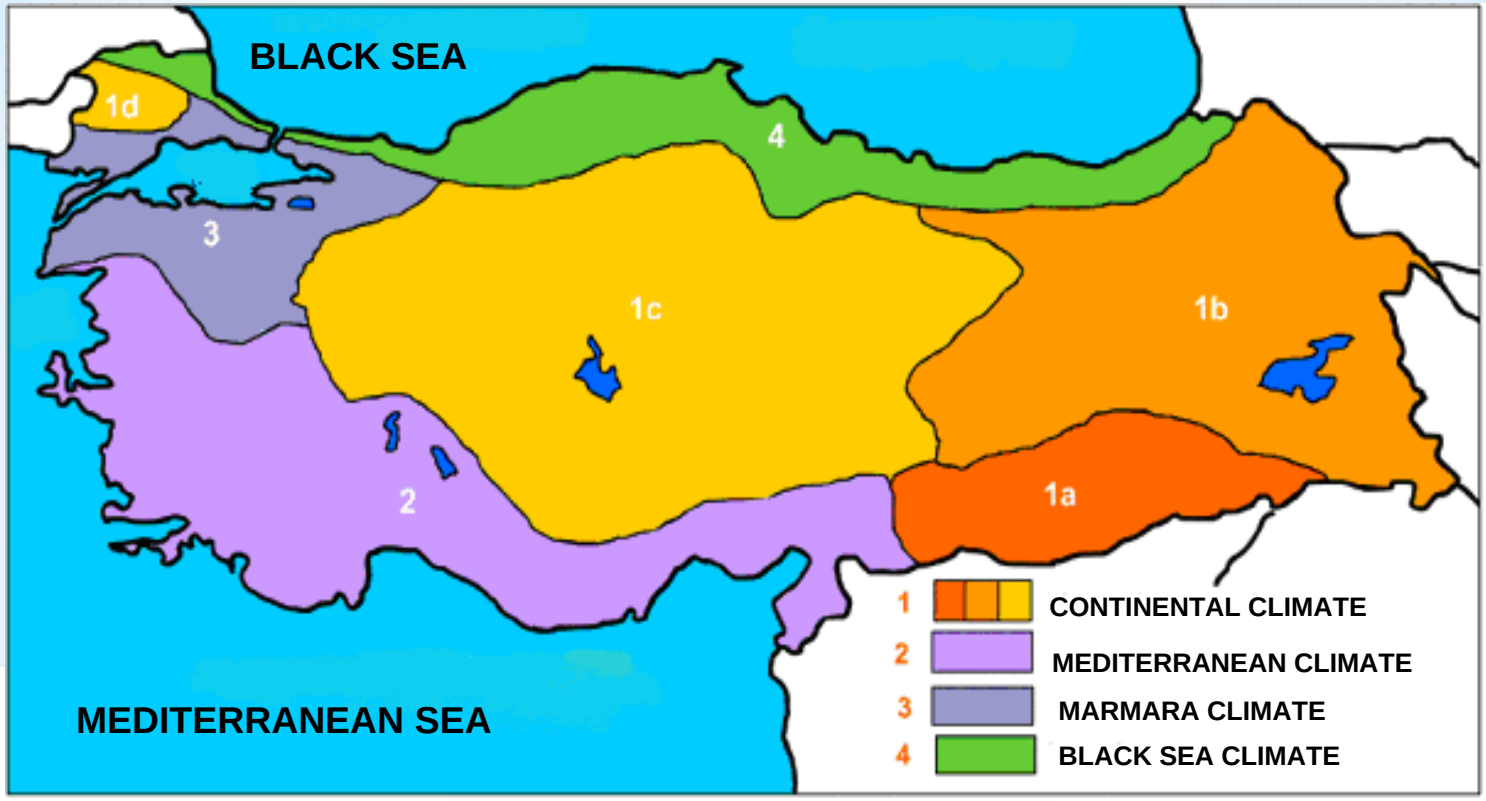

3) Marmara Climate: During winter, it is as hot as Mediterranean climate, but in summer not very rainy as much as Black Sea region. Winters are cold as continental climate and summers are hot and dry. Due to these features, Marmara climate has its position between continental Black Sea and Mediterranean Sea climates, as a transitional zone.

CLIMATE STRUCTURE IN TURKEY

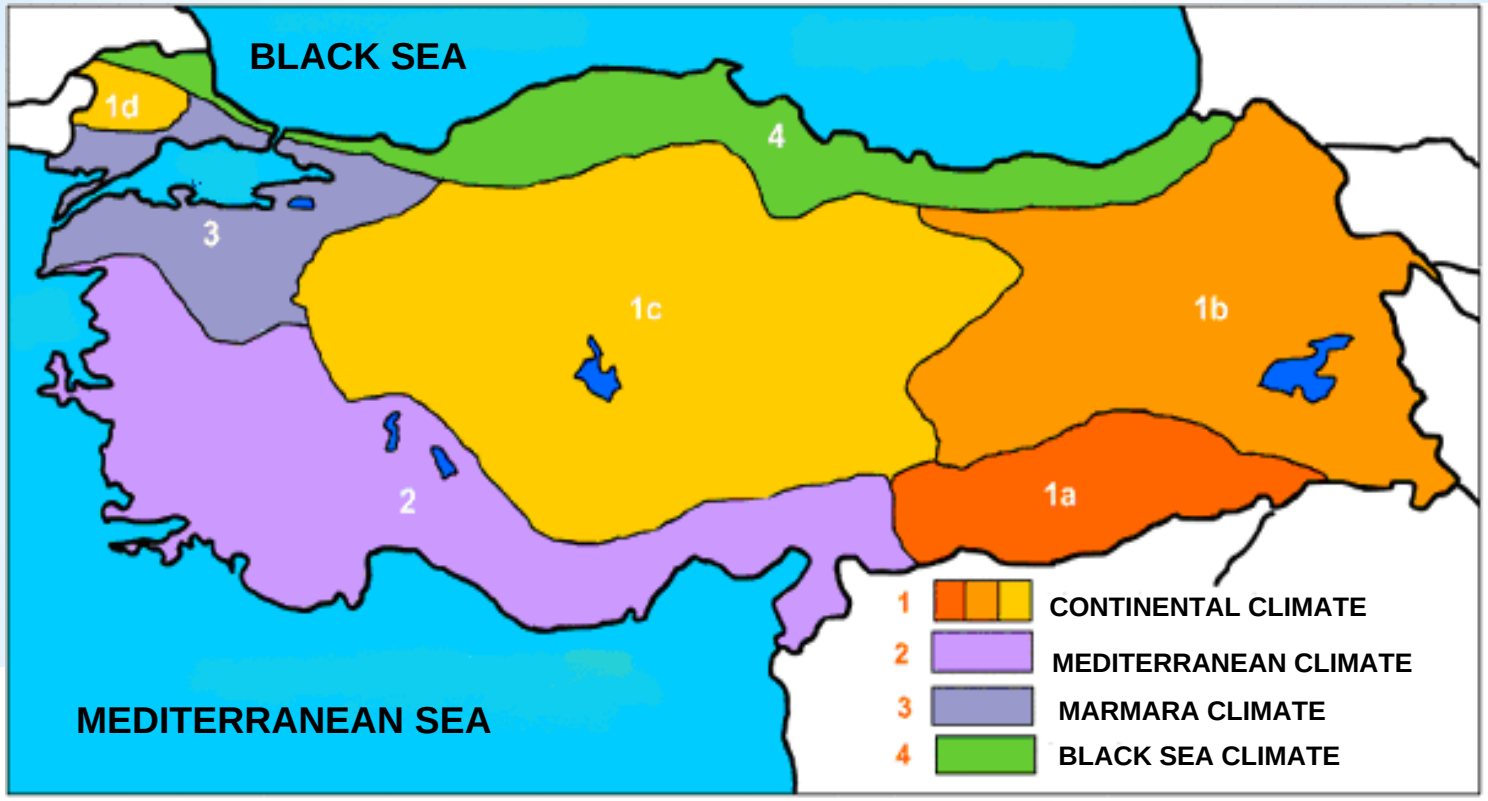

4) Black Sea Climate: Temperature differences between summer and winter are not very significant. Summers are rather cool, winters at coastal areas are warm but with snow and cold air at high elevation areas. Each season is rainy, and hence, there is not water scarcity or stress.

Observation Network in Turkey for This Study

Figure 1. Automated Weather Observation System (AWOS) station distribution in Turkey

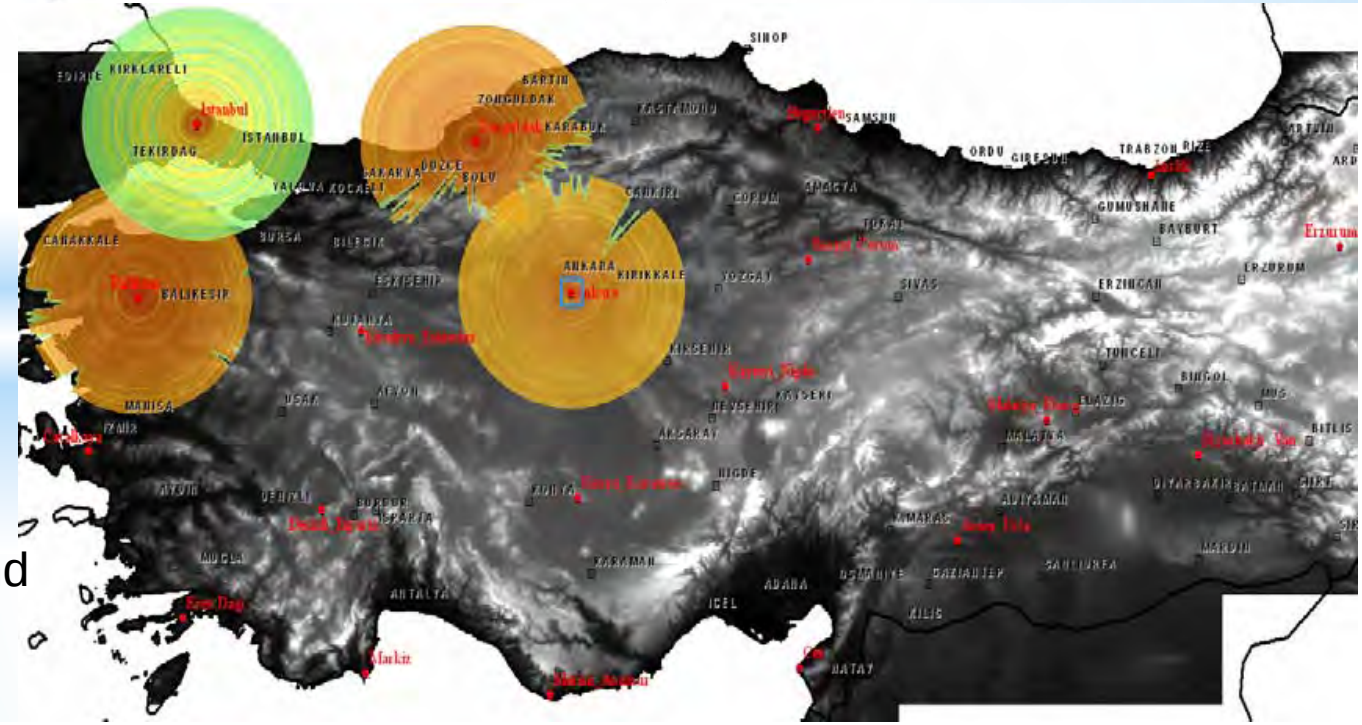

Figure 2. Radars sites and their coverage area in Turkey.

Defense Meteorological Satellites Program (DMSP)

The US Air Force is responsible for a program called the Defense Meteorological Satellites Program (DMSP) since the mid- 1960s.

ESTABLISHMENT OF THE CRD DATABASE

14 precipitation cases, which were observed between 2007 – 2009, are selected for establishing Turkish CDR database (Table 1).

Table 1. *Details of the 14 UW-NMS simulations*

START UP (spin off)		CASE STUDY		SIMULATION DURATION		
Date	hour	DATE	hour (start)	HOURS	Lat	Lon (E > 0)
2007/08/26	12.00	2007/08/27	00.00	60	40.28	32.64
2007/10/12	12.00	2007/10/13	00.00	60	40.13	28.27
2007/10/12	12.00	2007/10/13	00.00	60	40.28	32.64
2007/10/22	12.00	2007/10/23	00.00	60	40.13	28.27
2007/10/22	12.00	2007/10/23	00.00	60	40.28	32.64
2008/03/19	06.00	2008/03/19	18.00	60	40.13	28.27
2008/09/16	12.00	2008/09/17	00.00	60	40.28	32.64
2008/10/02	12.00	2008/10/03	00.00	60	40.15	28.28
2008/10/25	12.00	2008/10/26	00.00	60	40.13	28.28
2008/12/17	12.00	2008/12/18	00.00	60	40.13	28.27
2009/01/03	12.00	2009/01/04	00.00	60	40.15	28.28
2009/02/07	12.00	2009/02/08	00.00	60	40.15	28.28
2009/04/21	12.00	2009/04/22	00.00	48	40.15	28.28
2009/05/17	18.00	2009/05/18	06.00	54	40.15	28.28

Simulations Details

- University of Wisconsin – Non-hydrostatic Modeling System (UW-NMS) is used. This atmospheric model was developed by Prof. Dr. Gregory J. Tripoli.
- 3 nested, concentric and steady grids for each simulation.
- Domain 1: first and outer grid, 50 km resolution and 92 grid points.
- Domain 2: 10 km resolution and 92 grid points.
- Domain 3: 2 km resolution and 252 grid points.
- 35 vertical levels for all grids and maximum height is 18 km. In next slide, examples of UW-NMS rainfall rate and total water (ice + liquid) can be seen.

* NMS simulations

NMS model features:

Non-hydrostatic

Three nested domains:

1. Domain 1, 50 Km resolution with 92 grid points
2. Domain 2, 10 Km resolution with 92 grid points
3. Domain 3, 2 Km resolution with 252 grid points

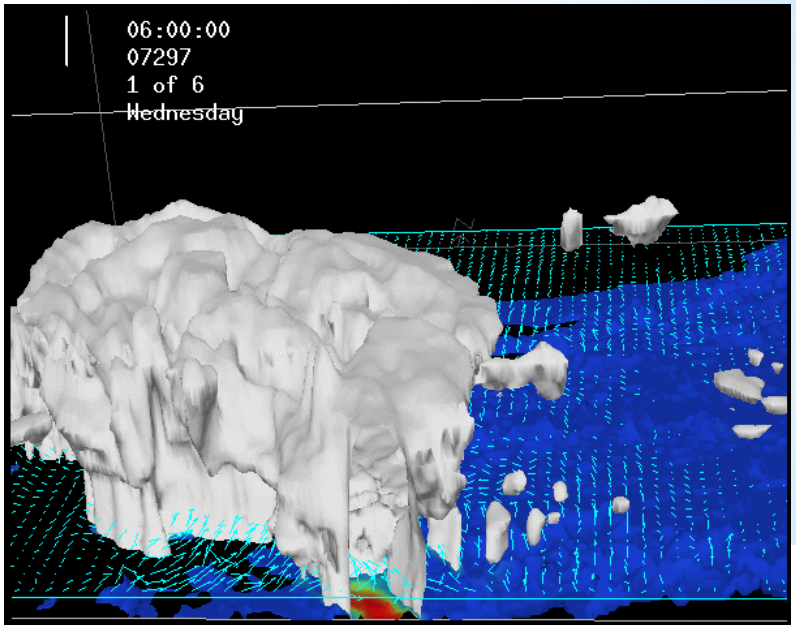

Domain 3; Example of UW-NMS total water (ice+liquid)

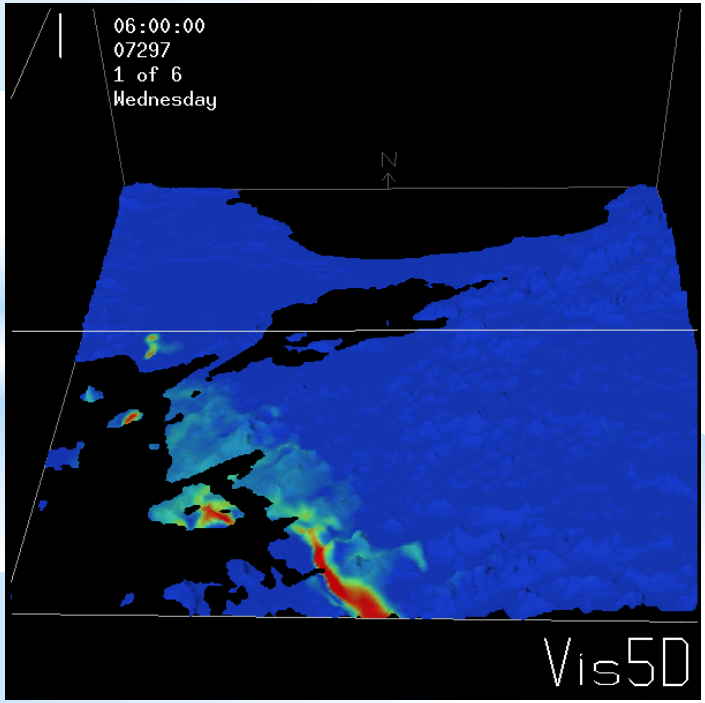

Domain 3; Corresponding UW-NMS model rainfall rate

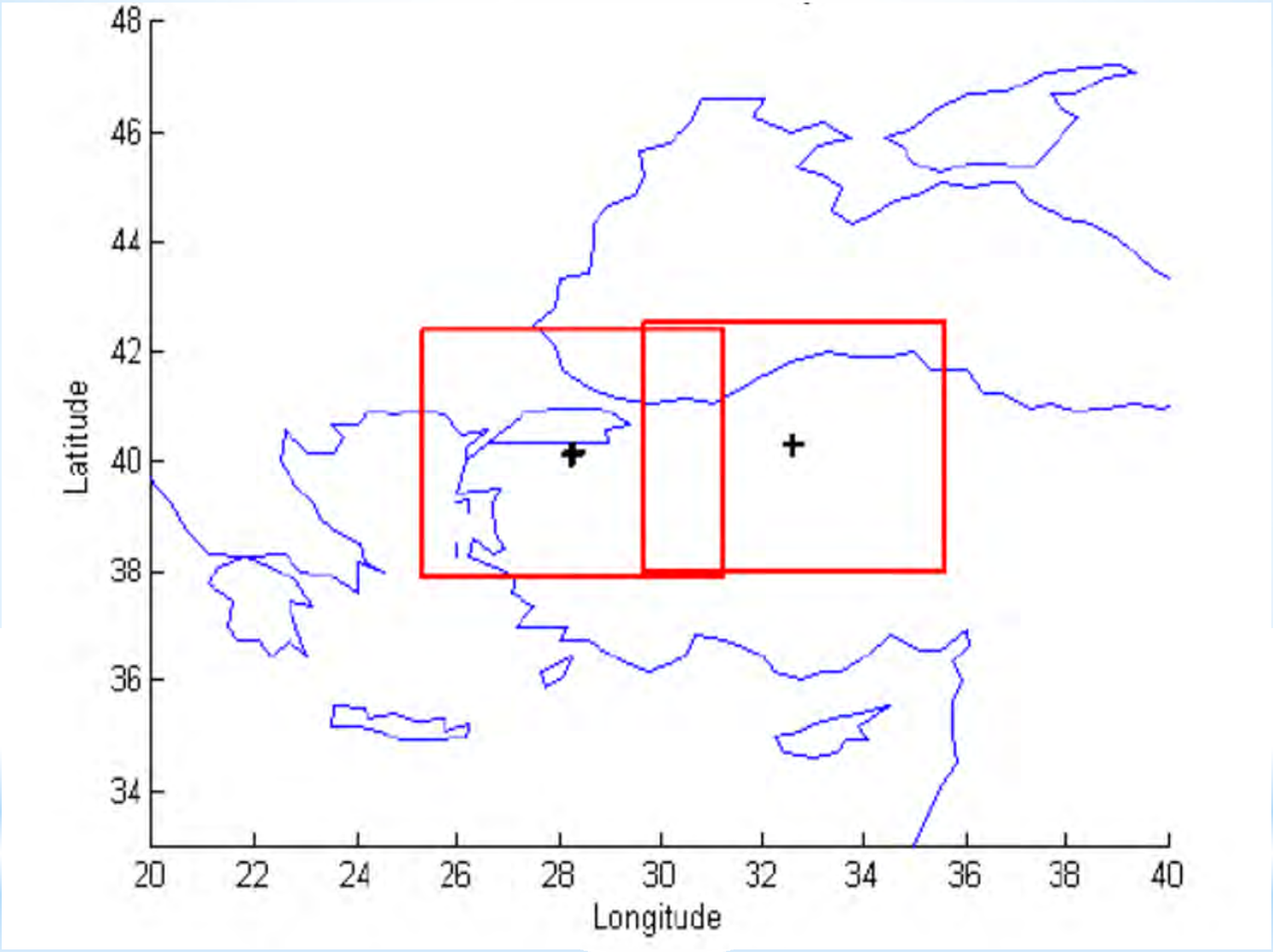

Red boxes show the inner domains (Domain 3) of UW-NMS simulation.

THE CDRD RETRIEVAL ALGORITHM

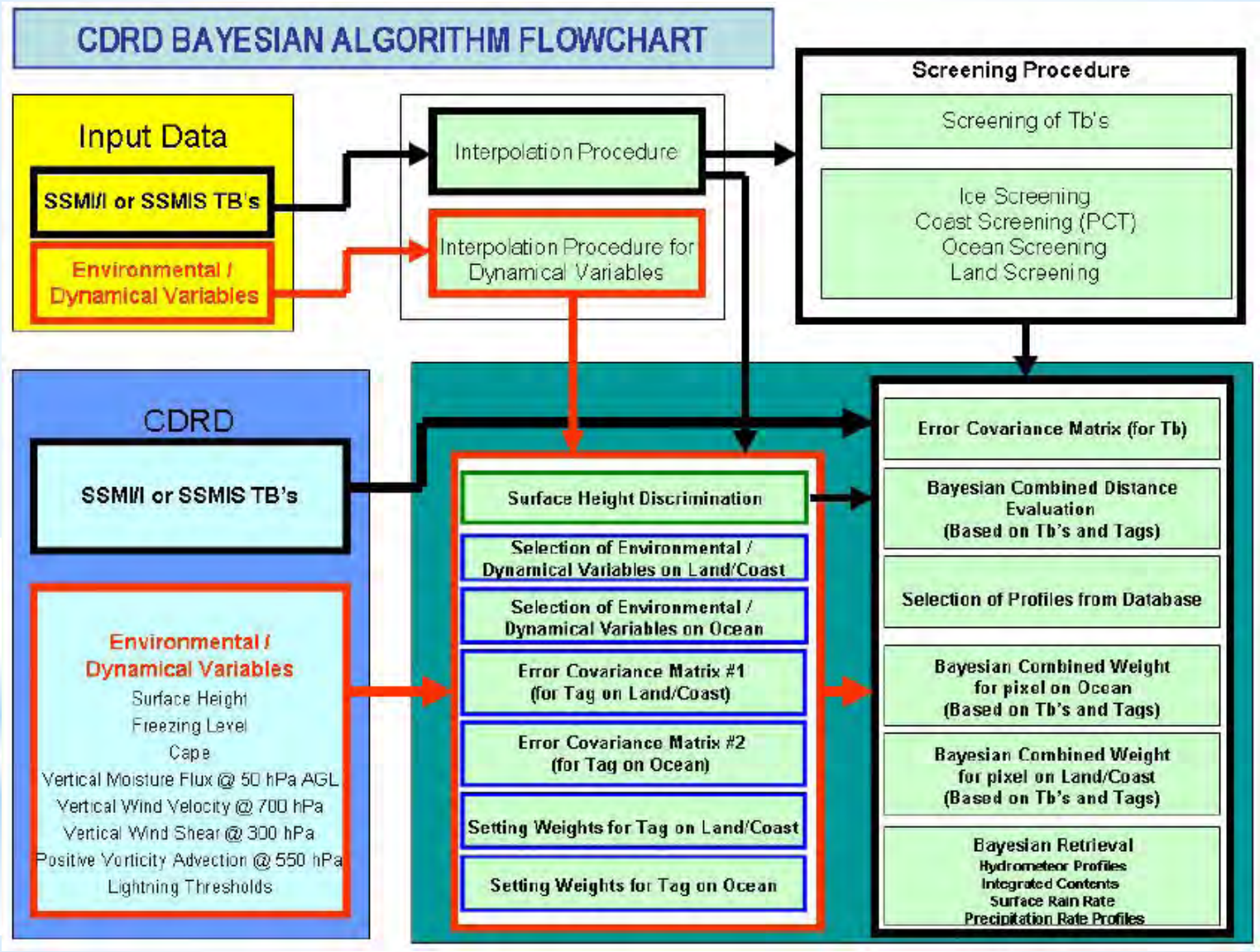

Block diagram of the CDRD Bayesian algorithm.

ANALYSIS PROCEDURE OF TURKISH CRD DATABASE

Table 3. Statistics indexes of simulated Brightness Temperatures (TBs) over land.

	Mean	Variance	Spread
Cloud Columnar Content (Kg m-2)	0.25	0.13	0 – 4.37
Rain Columnar Content (Kg m-2)	0.30	0.67	1 - 29.95
Graupel Columnar Content (Kg m-2)	0.07	0.28	0 – 40.15
Pristine Ice Columnar Content (Kg m-2)	0.62	1.87	0 – 18.01
Snow Columnar Content (Kg m-2)	0.34	0.40	0 – 4.80
Aggregate Columnar Content (Kg m-2)	0.04	0.02	0 – 4.66
Surface Rain Rate (mm hr-1)	0.97	10.85	1 – 184.69

TB19.35V (K) TB37.00H (K)
TB19.35H (K) TB85.00V (K)
TB22.24V (K) TB85.00H(K)
TB37.00V (K)
Vert-integrated cloud water path (kg/m**2)
Vert-integrated rain water path (kg/m**2)
vert-integrated graupel water path (kg/m**2)
vert-integrated pristine water path (kg/m**2)
vert-integrated snow water path (kg/m**2)
vert-integrated aggregates water path (kg/m**2)
Surface rain rate (mm/hr)
Surface pristine (mm/hr)
Surface aggregate (mm/hr)
Surface graupel (mm/hr)
Surface snow (mm/hr)
Profile number Latitude Longitude
Percent land Percent snow Percent
ice
Height of surface (km)
Iztop

Table 2. CRD database for SSMI/S components of each profile.

Figures 3 and 4 show the Turkish CRD database. It is possible to conclude that low water/ice contents and low precipitation are in the majority with a large variability in the cloud microphysical properties, which can be related to the coverage of different climatic regions, where types of precipitation and seasonal variations occur in Turkey.

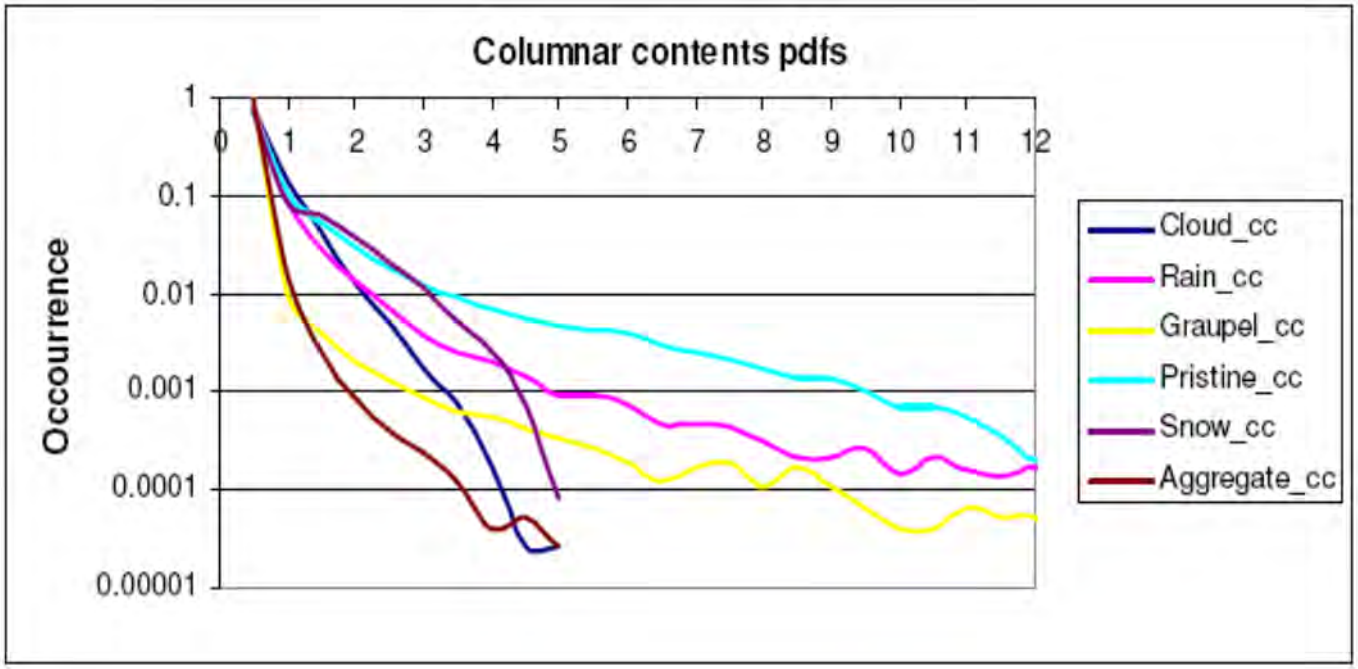

Figure 3. Probability Distribution Functions (PDFs) of the columnar contents (CC) of liquid and frozen hydrometeors within the Turkish CRD database.

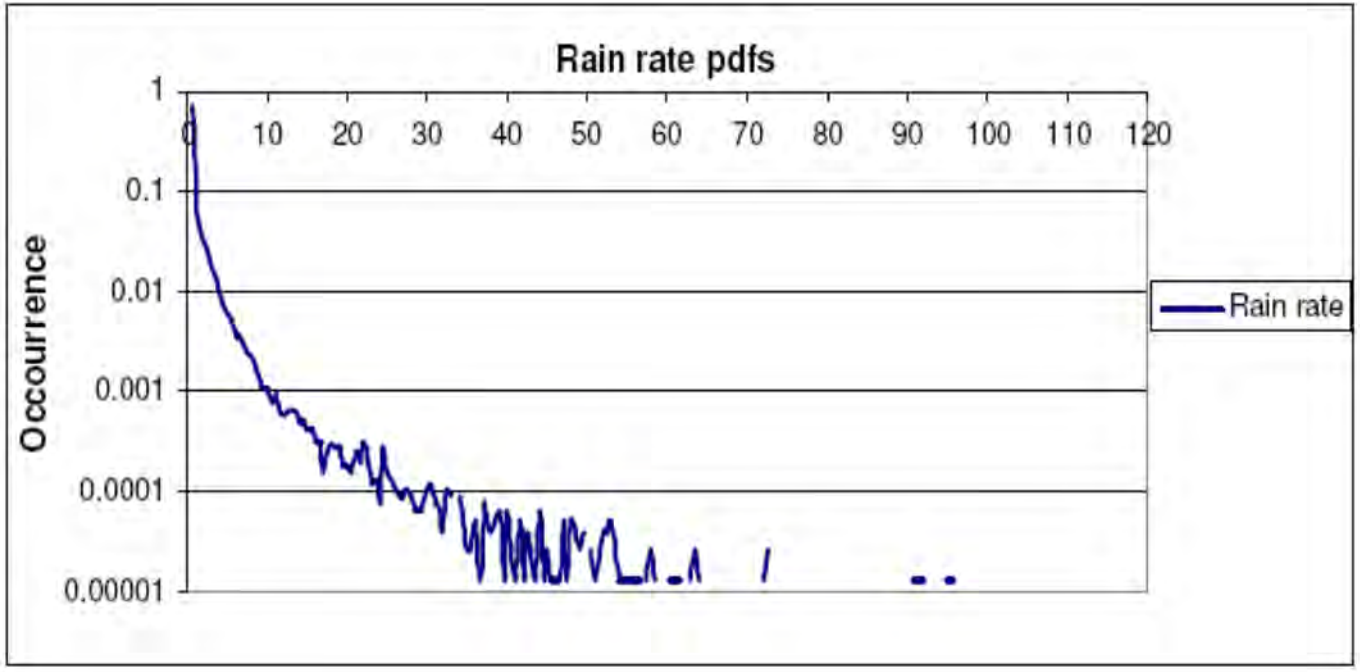

Figure 4. PDFs of liquid precipitation rates at the surface within the Turkish CRD database.

Figure 5 indicates that there is a large difference between the PDF peaks for land and ocean and it may be as a result of "cold" emission from the sea surface, which is coupled by land surfaces.

Additionally, for each frequency there appears a large difference over ocean between the two polarizations, and it may be due to the higher ocean emissivity at vertical polarization.

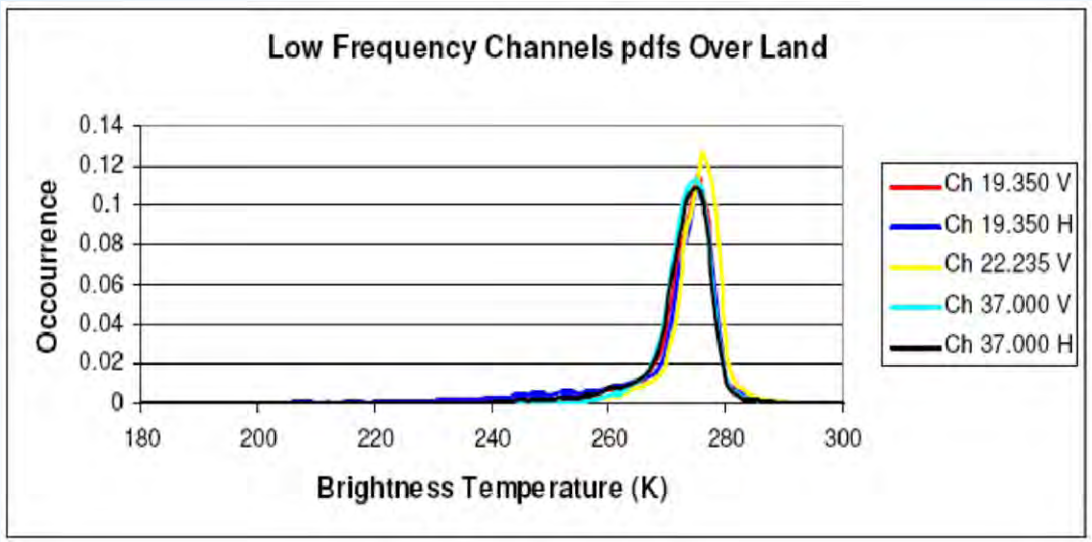

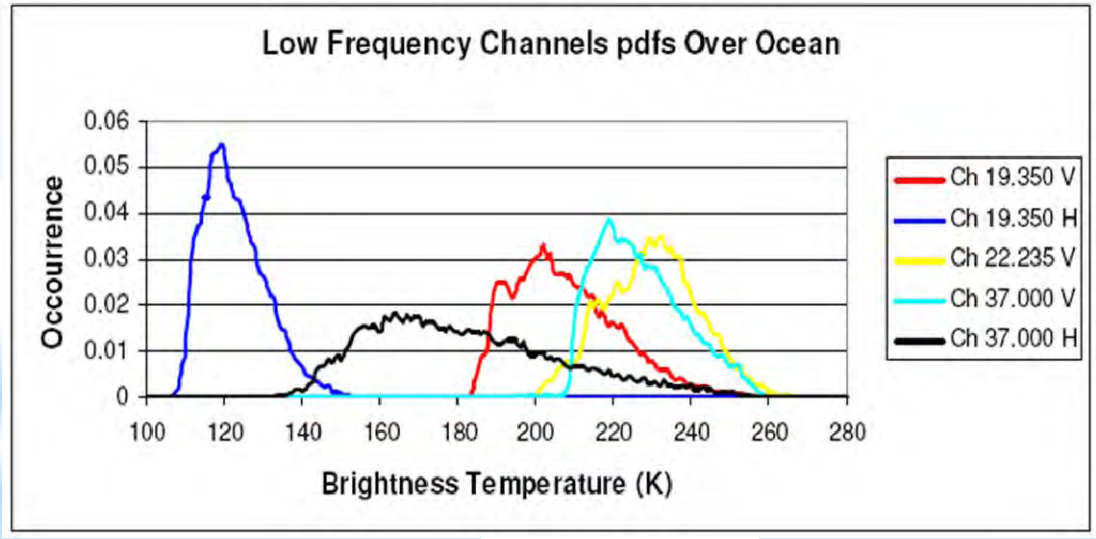

Figure 5. PDFs of the simulated upwelling TBs in the Turkish CRD database for the five low-frequency SSM/I – SSMIS window channels over land and ocean.

Figure 6 indicates the differences between land and ocean as well as the two polarizations, which are comparatively lower than for the low-frequency channels. This is as a result of much larger atmospheric contribution to the upwelling TBs.

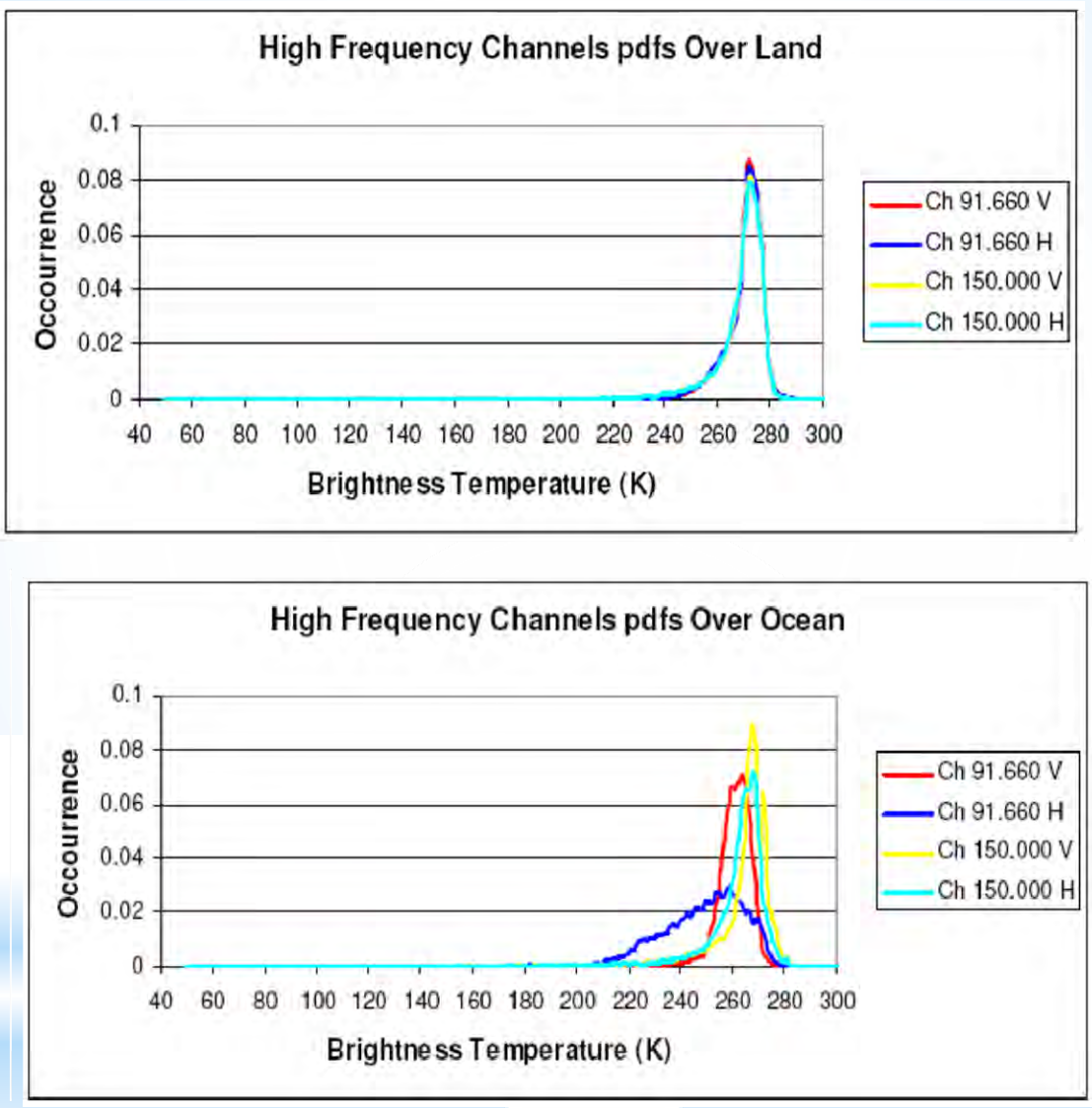

Figure 6. PDFs of the simulated upwelling TBs in the Turkish CRD database for the five high-frequency SSM/I – SSMIS window channels over land (left) and ocean (right).

In Figure 7, different colors are employed for the indication of the density concerning two databases around each 19-37 GHz "point". They are in terms of the log- occurrences at all 19-37 GHz couples as shown in the color bar. The simulations database are more consistent with the measurements apart from the long tail in the simulations (especially at 19 GHz).

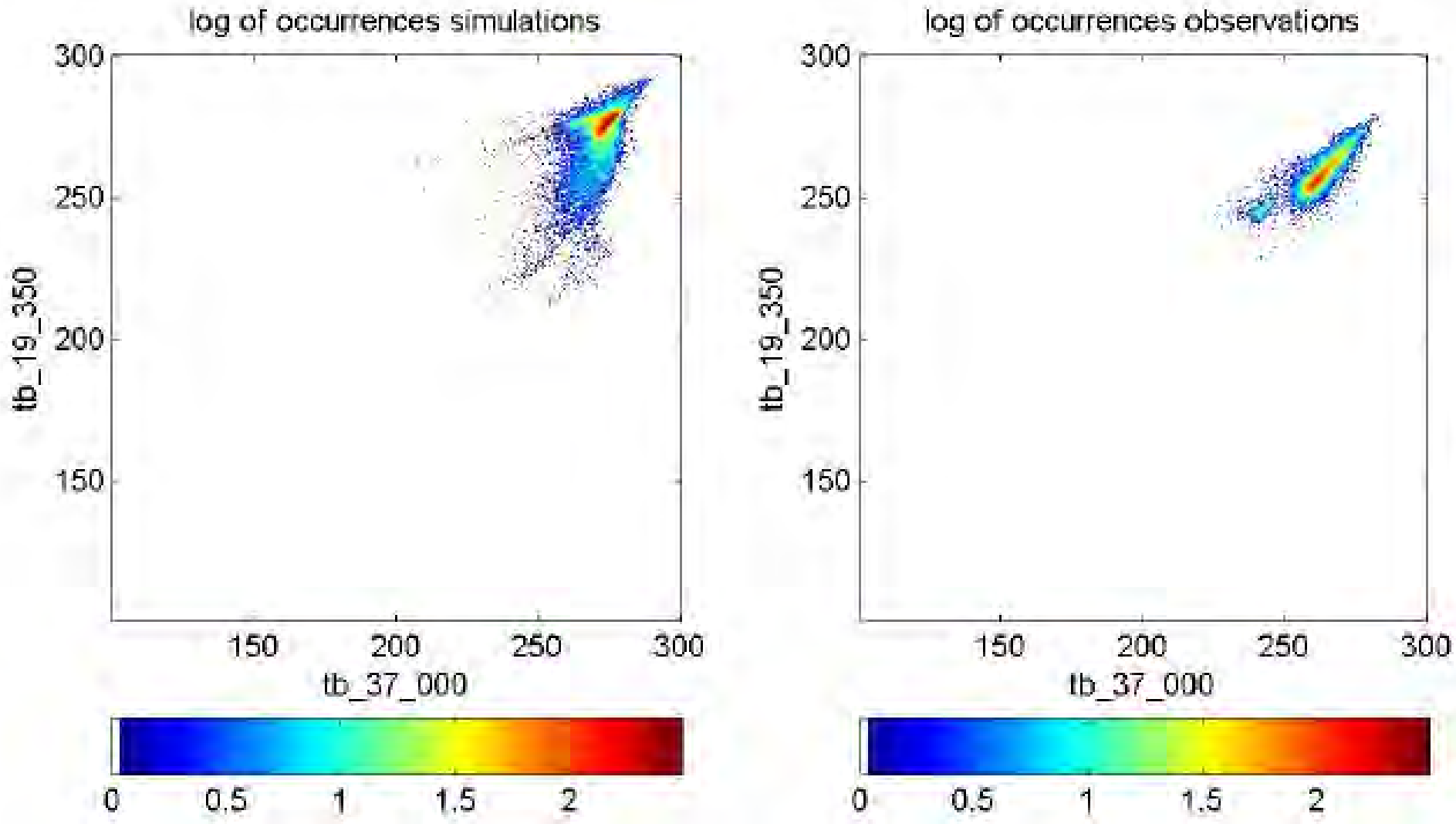

Figure 7. 19.35 GHz vs. 37 GHz scatter plot of the simulated TBs in the Turkish CRD database (left) and of the measured TBs in the SSM/I – SSMIS measurements database (right) – in both case, over land only.

Figure 8 represents in a better way than previous case in Figure 7 as for the consistency of the simulations with the measurements, because 50.3 GHz is less sensitive to surface characteristics than the lower window frequencies

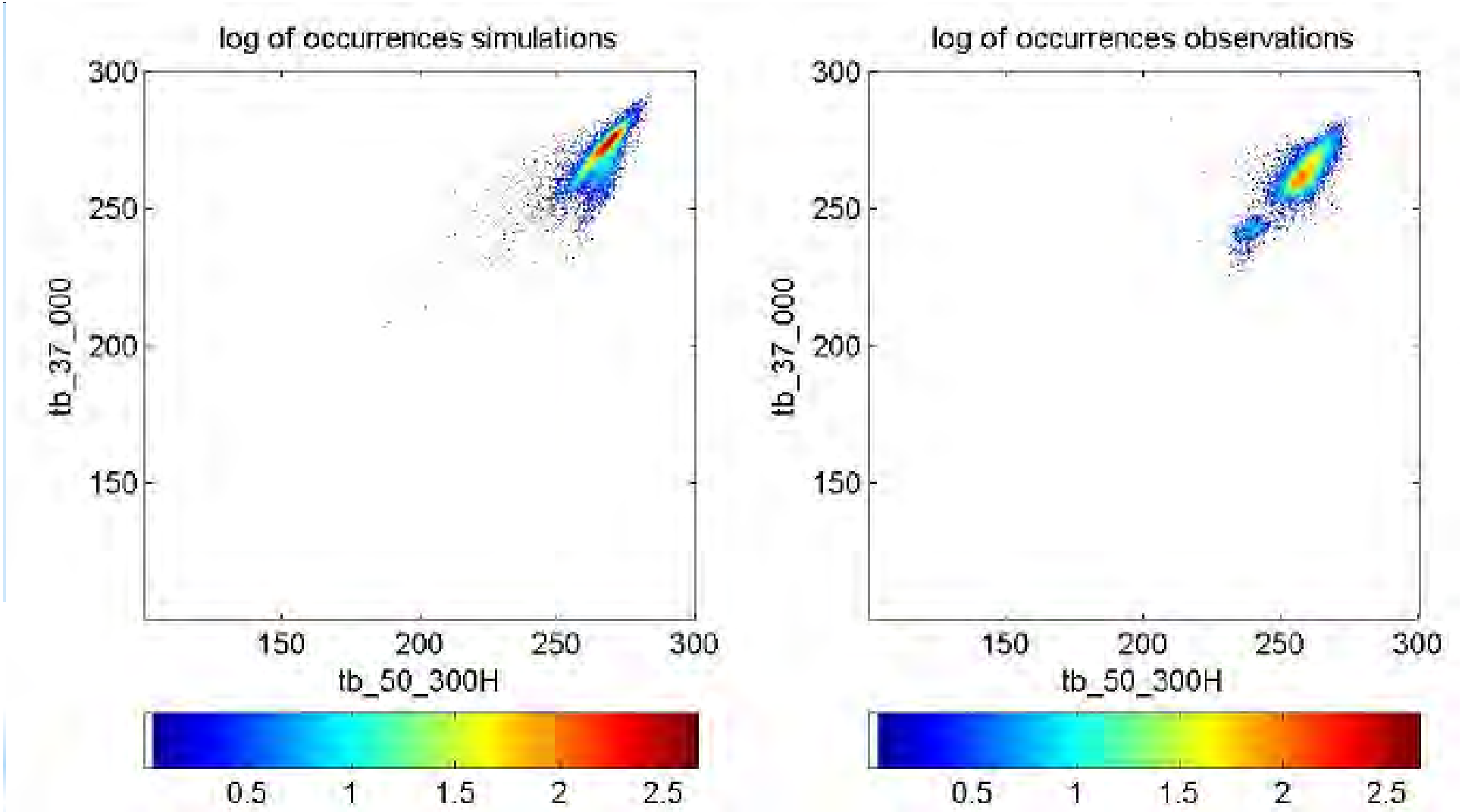

Figure 8. 37 GHz vs. 50.3 GHz scatter plot of SSMIS simulated (left) and measured TBs (right).

Surface emissivity does not impact significantly on the upwelling TBs at these high window frequencies (Figure 9). However, exceptions are only in thin cloud presence with very low precipitation. On the other hand, the overall consistency for simulations database shows the ice contents that are simulated rather properly by the UW-NMS model, where an appropriate ice scattering parameterizations is considered.

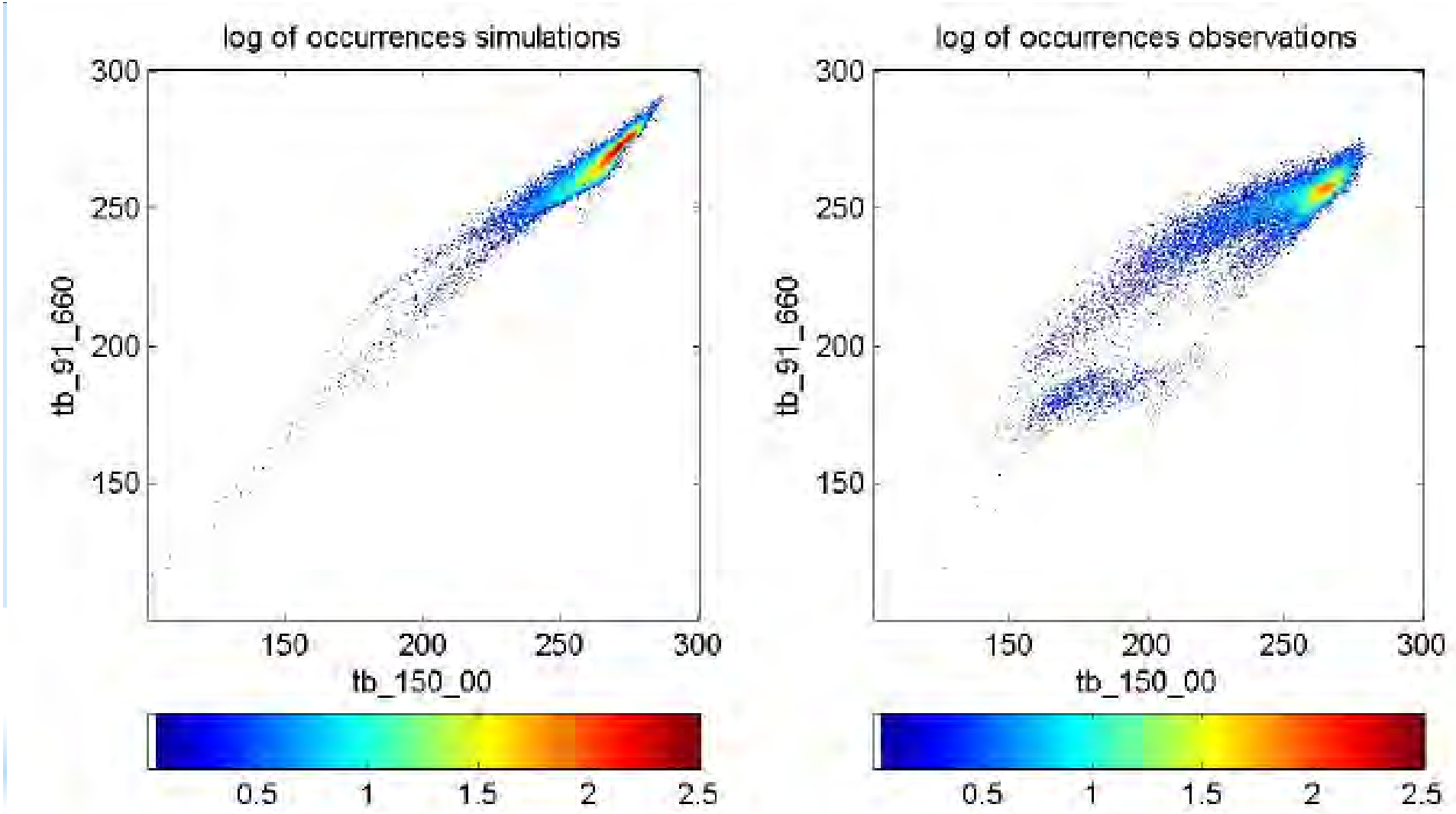

Figure 9. 91.66 GHz vs. 150 GHz scatter plot of SSMIS simulated (left) and measured TBs (right).

Figure 10 presents intense water vapor line absorption frequencies at 183.31 GHz. Herein, the surface emissivity impact is negligible but overall simulation consistency shows the ice contents, which are simulated by the UW-NMS model. Accordingly, appropriate ice scattering parameterizations are adopted especially at higher cloud portions.

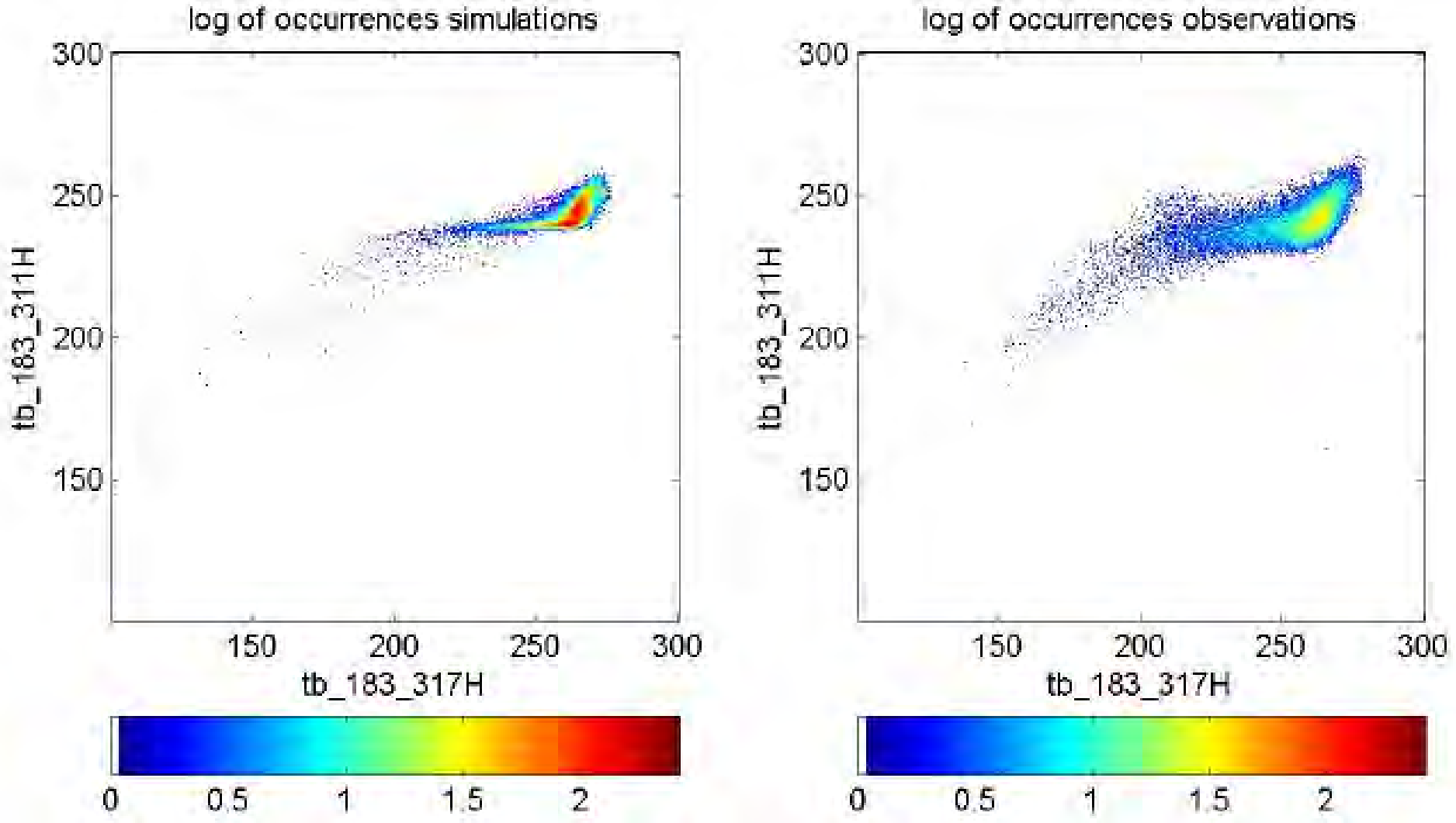

Figure 10. 183.31±3 GHz vs. 183.31±7 GHz scatterplot of SSMIS simulated (left) and measured TBs (right).

APPLICATION AND RESULTS

In Figure 11, scatter diagrams are obtained by considerations of 1x1 and 3x3 resolution rain rate retrievals versus radar values, respectively.

According to 45 degree line (red line), the overall regression line indicates overestimation results with a very significant variability deviations in Figure 11a.

On the other hand, in Figure 11b, 3x3 spatial filtering is applied to available data, and consequently, a better situation appears, but still the retrievals indicate overestimations.

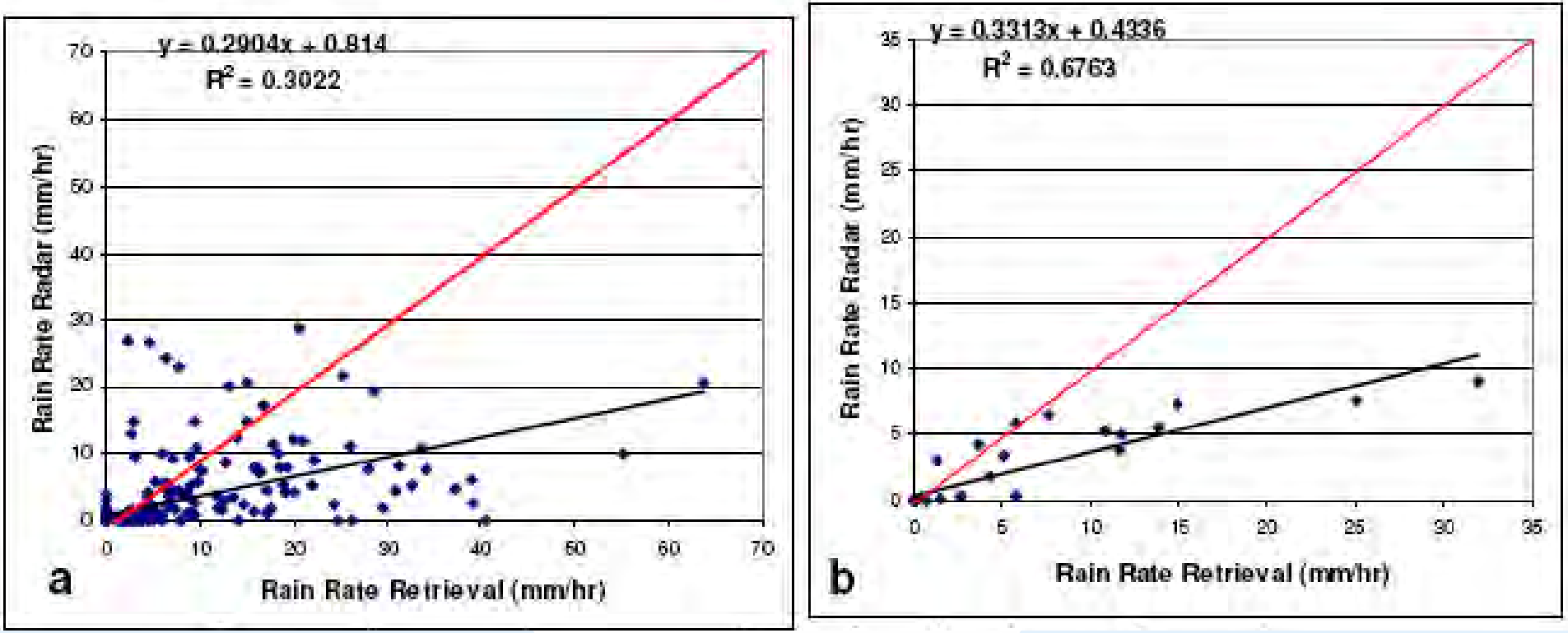

Figure 11. Scatter diagrams between radar and retrieval on 9 September 2009 at 03:40 GMT (a) original comparison, (b) after applying a 3x3 filter

Table 4 represents the statistical quantities while Table 5 shows the categorical statistics. Both statistical quantities and categorical statistics are satisfactory. Moreover, the retrieval and radar patterns have almost the same shape in Figure 12.

Table 4. Statistical features (9 September 2009 at 03:40 GMT)

Statistics	1X1 filter	3X3 filter
Mean Error	2.51	3.15
Mean absolute error	3.44	3.34
Mean squared error	63.49	40.57
Root mean square error	7.97	6.37
Standard deviation	7.57	5.64
Correlation coefficient	0.55	0.87
(Multiplicative) bias	2.15	2.25
URD-RMSE	15.78	21.08

Table 5. Rainfall occurrence indices (9 September 2009 at 03:40 GMT)

Categorical Statistics	1X1 filter	3X3 filter
POD	0.86	0.90
BIAS	0.99	0.90
FAR	0.13	0.00
CSI	0.77	0.90
HR	0.89	0.93
POFD	0.08	0.00

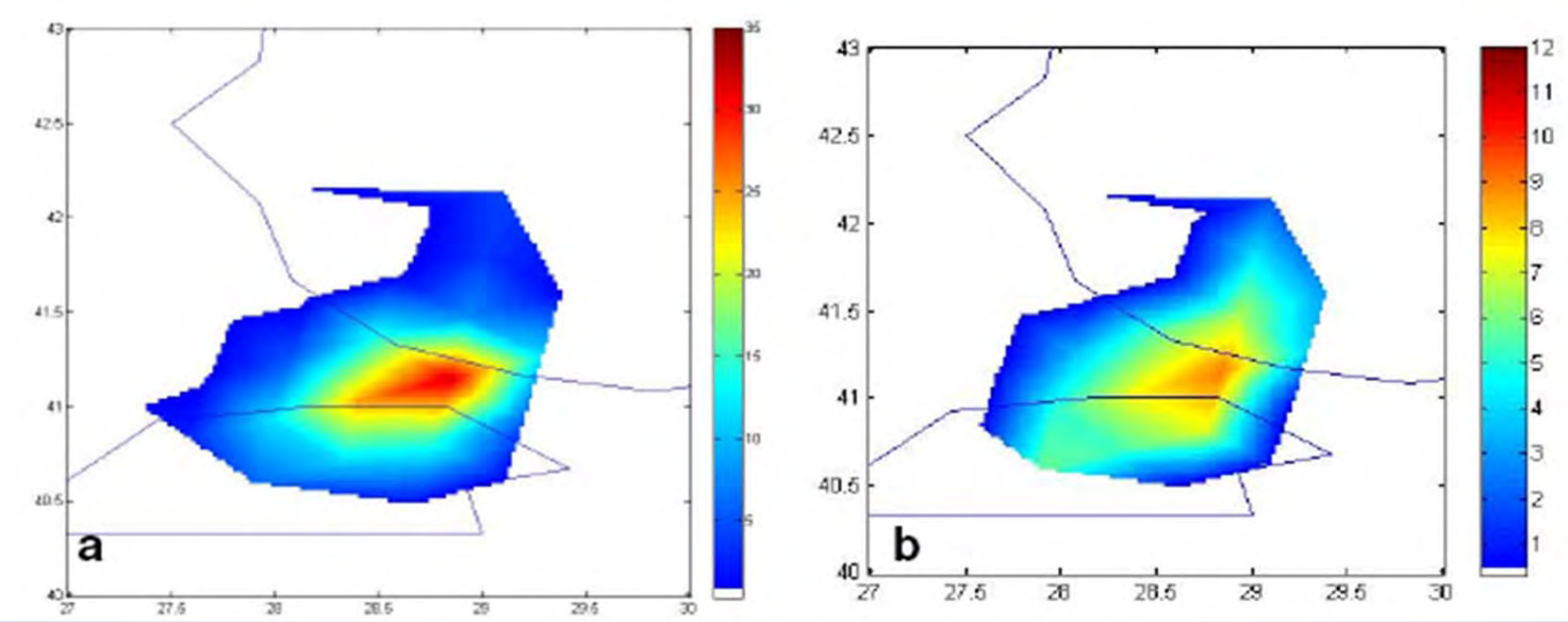

Figure 12. Patterns by using 3x3 filter on 9 September 2009 at 03:40 GMT (a) retrieval, (b) radar

Thanks for your patience…